Received: 16 February 2021 | Accepted: 12 March 2021

DOI: 10.1002/jsid.1011

SPECIAL SECTION PAPER

WILEY

Polarization-independent liquid crystal-based refractive index sensor

Zhiyong Yang, SID Student Member | **Tao Zhan, SID Student Member** | **Shin-Tson Wu, SID Fellow**

College of Optics and Photonics, University of Central Florida, Orlando, Florida, USA

Correspondence
Shin-Tson Wu, College of Optics and Photonics, University of Central Florida, Orlando, FL 32816, USA.
Email: swu@creol.ucf.edu

Funding information
Intel Corporation

Abstract

A polarization-independent refractive index (RI) sensor with a sensitivity of 50 nm/RIU is demonstrated. The proposed RI sensor simply consists of a liquid crystal (LC) polymeric polarization grating film and one glass substrate. The wavelength shift over the RI of the surrounding medium is investigated through anisotropic rigorous coupled-wave analysis. Such an LC-based polarization-independent RI sensor not only enables the usage of an unpolarized light source but also manifests a high sensitivity, offering great potential for the integration with display systems.

KEYWORDS

guided-mode resonance, polarization grating, polarization independent, refractive index sensor

1 | INTRODUCTION

Liquid crystals (LCs) have been widely used in flat panel displays[1,2] and phase-only spatial light modulators[3–6] due to their electrically tunable, large optical and dielectric anisotropies. In addition, their high sensitivity to the temperature, chemical environments, and pressure makes LCs a strong contender for sensors.[7] Among most of the sensing platforms, the LC-based waveguide is a promising method. The guided-mode resonance (GMR) can be excited when a diffracted order is phase matched to a leaky mode of the waveguide.[8] Such a resonance condition is very sensitive to the refractive index (RI) change; therefore, an LC-based RI sensor with a high sensitivity can be obtained.

However, most GMRs are polarization sensitive because of the different propagation constants for the transverse electric (TE) and transverse magnetic (TM) guided modes. Therefore, it poses limitation to the LC-based sensor where an unpolarized light source is used. Many efforts have been devoted to realizing polarization independence based on two-dimensional (2D) and one-dimensional (1D) gratings. Peng and Morris theoretically investigated and experimentally demonstrated the resonant anomalies in 2D gratings and polarization-independent narrowband GMRs.[9,10] Mizutani et al.[11] proposed a rhombic grating structure whose symmetric plane coincided with the incident plane to realize polarization-independent GMRs at an oblique incidence. Although a 2D grating can provide more degrees of freedom than its 1D counterpart, its geometrical structure and fabrication process are more complicated. Ding and Magnusson[12] designed a polarization-independent reflector based on a 1D single-layer waveguide grating with a large modulation depth, but the spectral bandwidth for the TE and TM polarizations was considerably different.

In this paper, a novel structure based on 1D LC polarization gratings (PGs) is proposed to realize the polarization-independent RI sensor. Compared with previous RI sensors, our method stands out due to its polarization independence and a relatively simple device structure. Specific structural parameters to realize the polarization-independent RI sensor are investigated and optimized, and an LC monomer is selected to present the polarization-independent RI sensor.

2 | POLARIZATION-INDEPENDENT RI SENSOR

The proposed RI sensor is simply composed of an LC-polymeric PG film on a glass substrate, as depicted in Figure 1. For a nematic LC, its anisotropy axis is along the direction of the LC directors. The propagation vector **k** lies in the x–z plane, and Λ and d are the grating periodicity and thickness, respectively. For a specific direction of the LC directors, the dielectric tensor $[\varepsilon]$ is given by[13]

$$\varepsilon = \begin{bmatrix} n_o^2 + (n_e^2 - n_o^2)\cos^2\phi & (n_e^2 - n_o^2)\sin\phi\cos\phi & 0 \\ (n_e^2 - n_o^2)\sin\phi\cos\phi & n_o^2 + (n_e^2 - n_o^2)\sin^2\phi & 0 \\ 0 & 0 & n_o^2 \end{bmatrix}, \quad (1)$$

where ϕ is the azimuthal orientation angle between the x axis and the projection of the LC directors on the x–y plane, the pretilt angle of the LC directors is assumed to be zero, and n_o and n_e is the LC ordinary and extraordinary RI, respectively. The LC directors periodically vary along the x axis in Figure 1, which can be mathematically expressed as $\phi(x) = \pi x/\Lambda$.

The proposed structure can function as a sensing device based on the mode matching: the real part of a mode propagation constant in a periodic leaky waveguide approaches the tangential propagation constant of a diffracted order, and strong resonance can result in a narrowband reflection peak. Incident waves can be coupled into certain waveguide modes due to the transverse momentum additionally provided by the grating; however, guided modes are not stable and thus become leaky due to the presence of the whole grating layer. The RI of surrounding medium can impact the mode propagation constant and thus determine the location of peak wavelength. Therefore, the variation of peak wavelength can be used for detecting a small change of RI.

In our device structure, the LC-polymeric PG acts as both a waveguide layer and a phase-matching medium. The LC-polymeric PG layer can be approximately treated as a uniform layer with an effective RI denoted by n_{eff}. Thus, this periodic anisotropic waveguide can be regarded as a three-layer homogeneous waveguide. Due to the grating diffraction, each diffracted order has a corresponding tangential propagation constant determined by the grating equation. When a diffracted order is phase matched to a leaky mode in the waveguide, the grating periodicity Λ, incident wavelength λ_0, and incident angle θ_{inc} are constrained by

$$\frac{2\pi}{\lambda_0}\max[n, n_1] < \left|\frac{2\pi}{\lambda_0}n_1 \sin\theta_{\text{inc}} - m\frac{2\pi}{\Lambda}\right| < \frac{2\pi}{\lambda_0}n_{\text{eff}}, \quad (2)$$

where n_1 is the RI of the glass substrate, which is set to be 1.52, n is the RI of the surrounding medium, and m is the diffraction order. Here, the target incident angle θ_{inc} is 0°. The geometrical parameters of the LC-polymeric PG are listed as follows: grating periodicity $\Lambda = 400$ nm and thickness $d = 1.591$ μm. A diacrylate LC monomer RM257 is selected as an example to illustrate our novel polarization-independent RI sensor. The ordinary and extraordinary refractive indices of RM257 are 1.508 and 1.687 at $\lambda_0 = 589$ nm, respectively.[14] To study the polarization dependence of this RI sensor, the polarization state of the incident light at normal incidence is expressed using Jones vector:

$$J = \begin{bmatrix} \cos\alpha \\ \sin\alpha \cdot e^{j\beta} \end{bmatrix}, \quad (3)$$

where $\tan(\alpha)$ represents the amplitude ratio of E_y to E_x and β is the relative phase angle between E_y and E_x. For each polarization state, the corresponding reflectance can be obtained via anisotropic rigorous coupled-wave

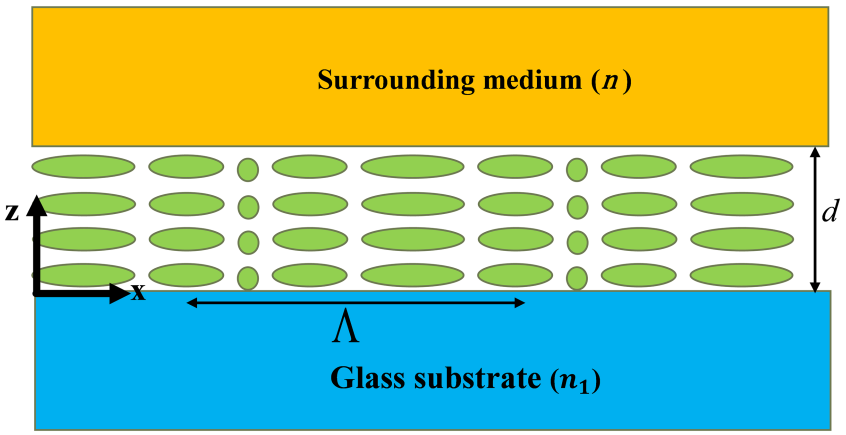

FIGURE 1 Device structure of the guided-mode resonance (GMR)-based refractive index (RI) sensor

analysis (RCWA).[15,16] The calculated reflectance at normal incidence is polarization independent, as shown in Figure 2.

Due to this polarization independency, unpolarized light sources can be employed. The RI of the surrounding medium is originally assumed to be equal to that of the glass substrate. When the unpolarized light is normally incident on the RI sensor, the peak wavelength of the reflected light can be detected, which is 625.42 nm as indicated by the green curve in Figure 3. The green curve also manifests a narrow bandwidth of $\Delta\lambda = 0.208$ nm. As the RI of surrounding medium varies, for example, due to the movement of biomolecules, the resonance wavelength also shifts. To quantify the performance of such a sensing device, the sensitivity and figure of merit (FOM) are introduced via $S = d\lambda/dn$ and FOM $= S/\Delta\lambda$, respectively.[17] The sensitivity describes the peak wavelength shift per RI unit with the unit of nm/RIU, thus a higher sensitivity allows for detecting a smaller RI change. The optimal sensitivity is dependent on the spectral bandwidth; therefore, FOM represents the maximum sensing capability or potential. According to Figure 3, the peak wavelength shifts 0.1 nm as the RI changes a step of 0.005. Thus, the sensitivity $S = 20$ nm/RIU and FOM $= 96$.

The RI sensor is also sensitive to the angle of incidence. Thus, its peak wavelength also shifts with the incident angle. Figure 4 manifests a narrow spectral and angular width, within which the reflectance is very high. Away from normal incidence, a degenerate reflectance versus wavelength curve is split into two branches, which means there are two wavelengths corresponding to the reflectance maximum at a fixed angle. This splitting phenomenon is predicted by Equation 2. To explore the origin of this polarization independence, the field distribution is also investigated via anisotropic RCWA. The field distribution in Figure 5A shows that when the light is incident from the bottom glass substrate ($z < 0$), the electric field within the subwavelength LC-polymeric PG ($0 < z < d$) is enhanced more than 20× due to the coupling between ±1 diffraction orders and evanescent waves. Due to normal incidence, two counterpropagating diffraction orders can be simultaneously excited, generating a standing-wave pattern along the x direction,[18] as illustrated in Figure 5A. When the incident wavelength is 620.00 nm, which is away from the resonance wavelength of 625.42 nm, Figure 5B depicts a rather weak resonant process where the electric field enhancement within the LC-polymeric PG is much less than that in Figure 5A. Thus, the field distribution in Figure 5B is almost equivalent to that in a single-layer uniform film sandwiched between two glass substrates.

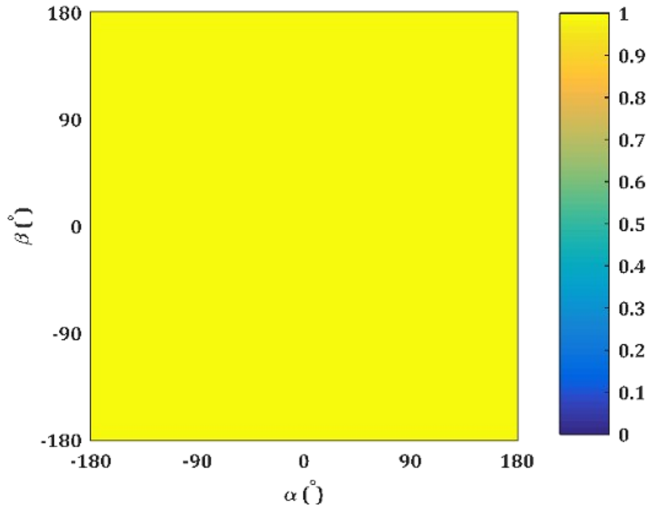

FIGURE 2 The reflectance for normally incident light with all polarization states defined by matrix J

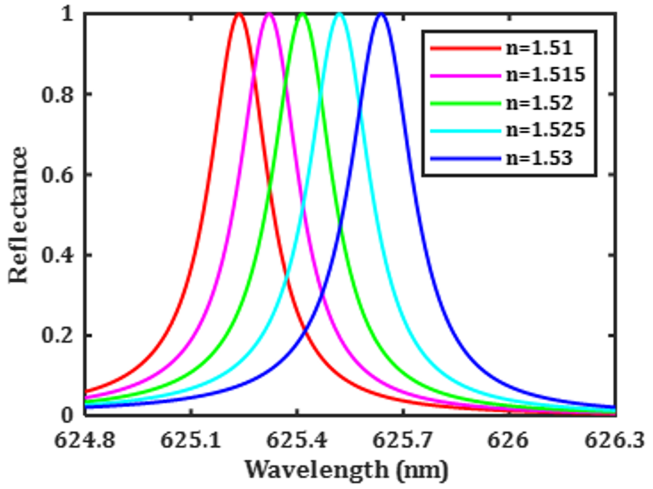

FIGURE 3 The wavelength shifts over the refractive index of the surrounding medium

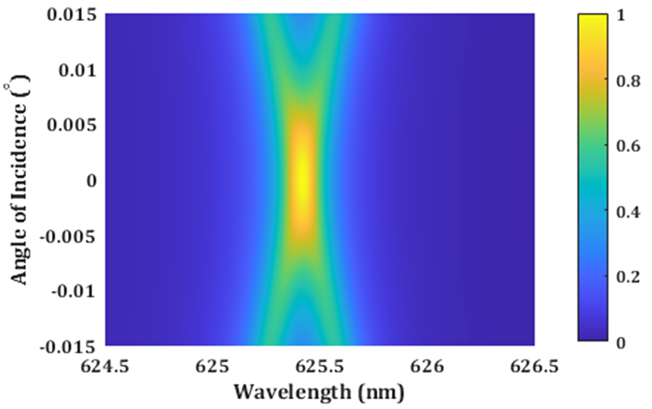

FIGURE 4 Angular and spectral responses of the refractive index (RI) sensor

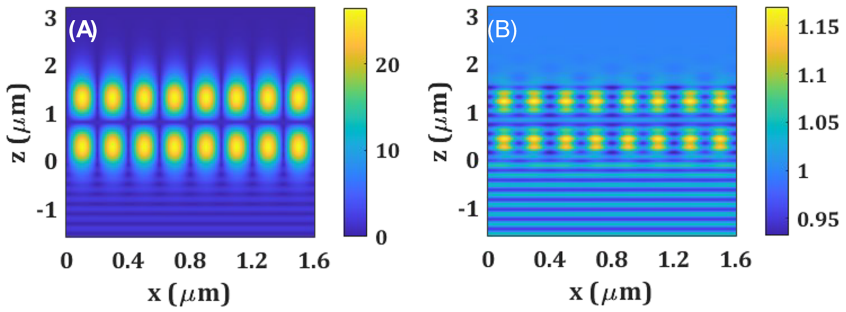

FIGURE 5 The relative electric field $|E/E_0|$ generated by rigorous coupled-wave analysis (RCWA) with light polarized along x axis: (A) at a resonance wavelength of 625.42 nm and (B) at a wavelength of 620.00 nm

In Figure 5, the mode type is still unknown because the field components are not revealed. Due to off-diagonal elements in the dielectric tensor, it is not possible to split the modes into a pure TE or TM mode, and thus, the modes are hybrid.[19] Figure 6 shows that right-handed circularly polarized (RCP) light and left-handed circularly polarized (LCP) light are coupled into the same HE_1 (TE_1 is dominant) hybrid mode. This polarization-independent coupling to the hybrid mode gives rise to the polarization-independent resonance location and bandwidth.

3 | IMPROVEMENT OF THE RI SENSOR

According to mode matching, the ±1 diffraction orders can be phase matched to several hybrid leaky modes at different resonance wavelengths.[20] For higher order modes, more beams will interfere with each other due to more reflection times at a given propagation distance. Thus, the spectral bandwidth corresponding to higher order modes becomes narrower. If a higher order mode is employed to detect a small RI change, a higher FOM can be obtained. Figure 7 shows the reflectivity verses the wavelength ranging from 611.5 to 614 nm as the RI is changed via a step of 0.005. Compared with Figure 3, a narrower bandwidth of 0.0588 nm is obtained, and the enlarged peak wavelength shift is 0.25 nm. Thus, the sensitivity S is 50 nm/RIU, and the FOM is as high as 850. To identify this corresponding higher order mode, the field analysis is conducted, and Figure 8 manifests that this mode has two minimum values, corresponding to the second-order mode. The mode type remains the same as the HE hybrid mode, and thus, the mode can be called HE_2.

Considering making a real device, the detailed fabrication process has been reported previously.[21] Here, we only briefly outline the procedures. The first step is to spin coat a PAL on a cleaned glass substrate. Next step is to expose the PAL using a linearly polarized light with spatial-variant polarization directions. Then, an

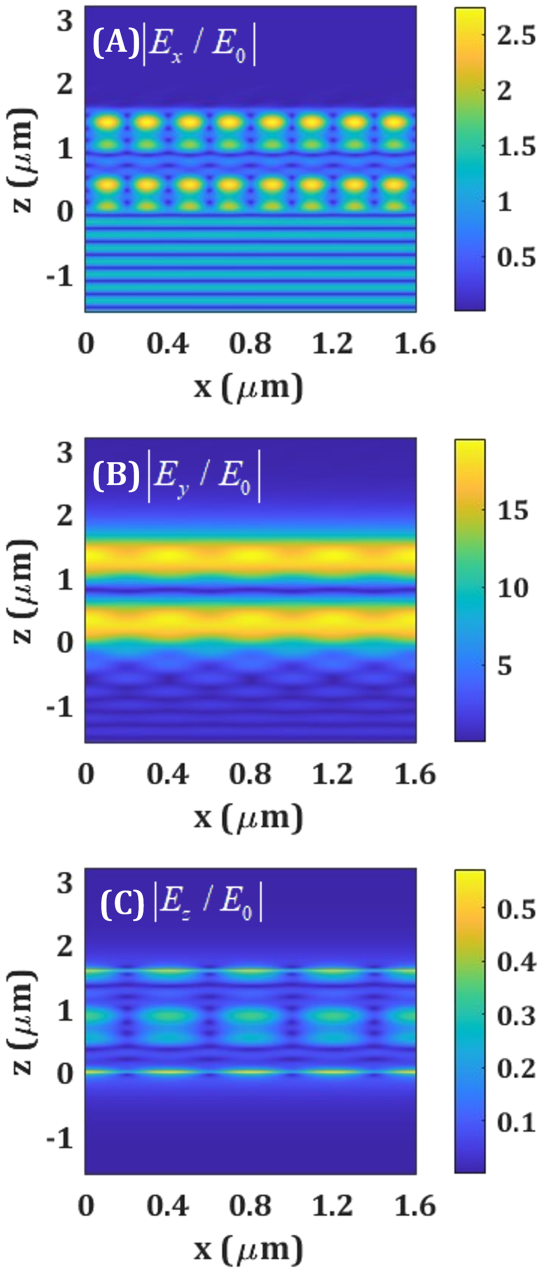

FIGURE 6 The relative electric field of (A) $|E_x/E_0|$, (B) $|E_y/E_0|$, and (C) $|E_z/E_0|$ for right-handed circularly polarized (RCP) and left-handed circularly polarized (LCP) lights at a resonance wavelength of 625.42 nm

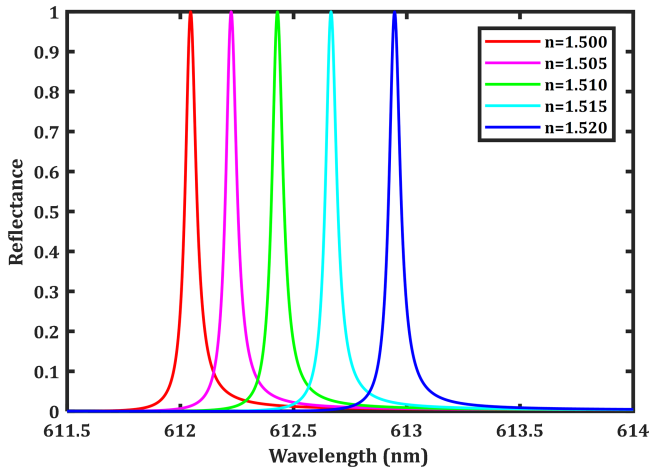

FIGURE 7 The wavelength shift versus the refractive index change of the surrounding medium

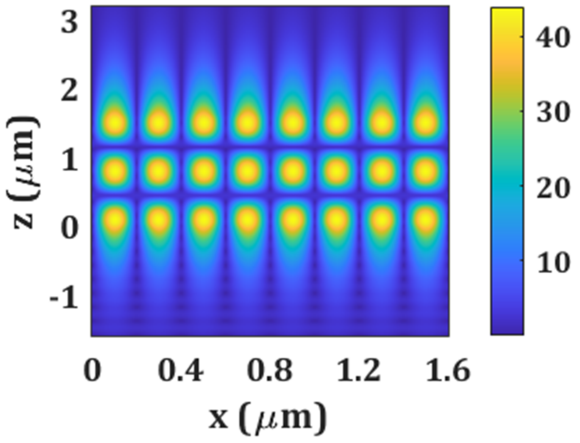

FIGURE 8 The relative electric field $|E/E_0|$ generated by rigorous coupled-wave analysis (RCWA) with light polarized along the x axis at a resonance wavelength of 612.94 nm

LC-reactive mesogen precursor is prepared by mixing solvent, monomer, photoinitiator, and surfactant together. The mixture is spin coated on the patterned PAL to align the LC directors. Finally, an ultraviolet light is used to polymerize the mixture. The same steps can be applied for depositing more polymerized layers to achieve a thicker film.

4 | CONCLUSION

A polarization-independent RI sensor has been demonstrated, which frees from the limitation for a polarized illumination light source. The sensitivity of this RI sensor can be further increased by employing higher order modes. The RI sensor can be also used for fluorescence enhancement due to the electric field enhancement. Traditional LC-based display devices can also be applied for sensing applications with a high sensitivity and polarization independence.

ACKNOWLEDGMENT

The authors are indebted to the partial financial support of Intel Corporation.

ORCID

Zhiyong Yang https://orcid.org/0000-0002-7181-7443
Shin-Tson Wu https://orcid.org/0000-0002-0943-0440

REFERENCES

1. Huang Y, Hsiang EL, Deng MY, Wu ST. Mini-LED, micro-LED and OLED displays: present status and future perspectives. Light Sci Appl. 2020;9(1):105.
2. Chen H, Lee JH, Lin BY, Chen S, Wu ST. Liquid crystal display and organic light-emitting diode display: present status and future perspectives. Light Sci Appl. 2018;7(3):17168.
3. Fan-Chiang KH, Huang SH, Shen CY, et al. Analog LCOS SLM devices for AR display applications. J Soc Inf Disp. 2020;28:581–590.
4. Pérez-Cabré E, Millán MS. Liquid crystal spatial light modulator with optimized phase modulation ranges to display multiorder diffractive elements. Appl Sci. 2019;9(13):2592.
5. Huang Y, Liao E, Chen R, Wu ST. Liquid-crystal-on-silicon for augmented reality displays. Appl Sci. 2018;8(12):2366.
6. Zou J, et al. Fast-response liquid crystal for spatial light modulator and LiDAR applications. Crystals. 2021;11(2):93.
7. Esteves C, Ramou E, Porteira AR, Moura Barbosa AJ, Roque AC. Seeing the unseen: the role of liquid crystals in gas-sensing technologies. Adv Optical Mater. 2020;8(11):1902117.
8. Quaranta G, Basset G, Martin OJ, Gallinet B. Recent advances in resonant waveguide gratings. Laser Photon Rev. 2018;12(9):1800017.
9. Peng S, Morris GM. Resonant scattering from two-dimensional gratings. J Opt Soc Am A. 1996;13(5):993–1005.
10. Peng S, Morris GM. Experimental demonstration of resonant anomalies in diffraction from two-dimensional gratings. Opt Lett. 1996;21(8):549–551.
11. Mizutani A, Kikuta H, Nakajima K, Iwata K. Nonpolarizing guided-mode resonant grating filter for oblique incidence. J Opt Soc Am A. 2001;18(6):1261–1266.
12. Ding Y, Magnusson R. Resonant leaky-mode spectral-band engineering and device applications. Opt Express. 2004;12(23):5661–5674.
13. Huang Y, Wu TX, Wu ST. Simulations of liquid-crystal Fabry-Perot etalons by an improved 4×4 matrix method. J Appl Phys. 2003;93(5):2490–2495.
14. Chien CY, Sheu CR. Doping liquid crystal cells with photocurable monomer via holographic exposure to realize optical-scattering-free infrared phase modulators with fast response time. Crystals. 2017;7(7):208.
15. Moharam MG, Gaylord TK. Rigorous coupled-wave analysis of planar-grating diffraction. J Opt Soc Am A. 1981;71(7):811–818.

16. Xiong J, Wu ST. Rigorous coupled-wave analysis of liquid crystal polarization gratings. Opt Express. 2020;28(24): 35960–35971.
17. Lan G, Zhang S, Zhang H, et al. High-performance refractive index sensor based on guided-mode resonance in all-dielectric nano-silt array. Phys Lett A. 2019;383(13):1478–1482.
18. Wei C, Liu S, Deng D, Shen J, Shao J, Fan Z. Electric field enhancement in guided-mode resonance filters. Opt Lett. 2006; 31(9):1223–1225.
19. Beeckman J, James R, Fernández FA, De Cort W, Vanbrabant PJ, Neyts K. Calculation of fully anisotropic liquid crystal waveguide modes. J Lightwave Technol. 2009;27(17): 3812–3819.
20. Yang Z, Zhan T, Wu ST. Polarization independent guided-mode resonance in liquid crystal-based polarization gratings. OSA Contin. 2020;3(11):3107–3115.
21. Zhan T, Lee YH, Tan G, et al. Pancharatnam–Berry optical elements for head-up and near-eye displays. J Opt Soc Am B. 2019;36(5):D52–65.

AUTHOR BIOGRAPHIES

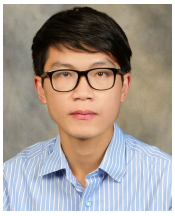

Zhiyong Yang received his BS degree in Optoelectronic Engineering from Chongqing University in 2017 and is currently working toward a PhD degree from the College of Optics and Photonics, University of Central Florida. His current research interests include liquid crystal-based sensors, mini-LED backlight, OLED display, and micro-LED display.

Tao Zhan received his BS degree in Physics from Nanjing University in 2016 and is currently working toward a PhD degree from the College of Optics and Photonics, University of Central Florida. His current research interests include near-eye display, planar optics, and diffractive optics.

Shin-Tson Wu is a Pegasus Professor at the College of Optics and Photonics, University of Central Florida. He is among the first six inductees of the Florida Inventors Hall of Fame (2014) and a Charter Fellow of the National Academy of Inventors (2012). He is a fellow of the IEEE, OSA, SID, and SPIE and an honorary professor at Nanjing University (2013) and at National Chiao Tung University (2018). He is the recipient of 2014 OSA Esther Hoffman Beller Medal, 2011 SID Slottow-Owaki Prize, 2010 OSA Joseph Fraunhofer Award, 2008 SPIE G. G. Stokes Award, and 2008 SID Jan Rajchman Prize.

How to cite this article: Yang Z, Zhan T, Wu S-T. Polarization-independent liquid crystal-based refractive index sensor. *J Soc Inf Display*. 2021;29:305–310. https://doi.org/10.1002/jsid.1011